

ADA053164

AFGL-TR-77-0288
AIR FORCE GEOPHYSICS IN GEOPHYSICS, NO. 380

12



Modeling of the Geosynchronous Orbit Plasma Environment - Part I

HENRY B. GARRETT, Capt. USAF

14 December 1977

Approved for public release; distribution unlimited.

SPACE PHYSICS DIVISION PROJECT 7661
AIR FORCE GEOPHYSICS LABORATORY
HANSCOM AFB, MASSACHUSETTS 01731

AIR FORCE SYSTEMS COMMAND, USAF

Best Available Copy



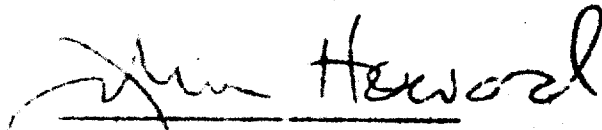
DDC
APR 23 1978
F

Best Available Copy

This report has been reviewed by the ESD Information Office (OI) and is releasable to the National Technical Information Service (NTIS).

This technical report has been reviewed and is approved for publication.

FOR THE COMMANDER


Chief Scientist

Qualified requestors may obtain additional copies from the Defense Documentation Center. All others should apply to the National Technical Information Service.

⑨ Air Force Surveys in geophysics

②

6.7

Unclassified

SECURITY CLASSIFICATION OF THIS PAGE (When Data Entered)

REPORT DOCUMENTATION PAGE		READ INSTRUCTIONS BEFORE COMPLETING FORM	
1. REPORT NUMBER AFGL-TR-77-0288-PT-1, AFGL-AFSG-380-PT-1		2. REPORT CATEGORY NUMBER	
3. TITLE (and Subtitle) MODELING OF THE GEOSYNCHRONOUS ORBIT PLASMA ENVIRONMENT, PART I.		4. DATE OF REPORT & PERIOD COVERED Scientific, Intern.	
5. AUTHOR(s) Henry B. Garrett, Capt, USAF		6. PERFORMING ORG. REPORT NUMBER AFSG No. 380 ✓	
7. PERFORMING ORGANIZATION NAME AND ADDRESS Air Force Geophysics Laboratory (PHG) Hanscom AFB Massachusetts 01731		8. CONTRACT OR GRANT NUMBER(s)	
9. CONTROLLING OFFICE NAME AND ADDRESS Air Force Geophysics Laboratory (PHG) Hanscom AFB Massachusetts 01731		10. PROGRAM ELEMENT, PROJECT, TASK AREA & WORK UNIT NUMBERS 76610801 62101F	
11. MONITORING AGENCY NAME & ADDRESS (if different from Controlling Office) 16. 76611 / 17. 78 /		12. REPORT DATE 14 Dec 1977	
		13. NUMBER OF PAGES 46 72/46P	
		14. SECURITY CLASS. (of this report) Unclassified	
		15a. DECLASSIFICATION/DOWNGRADING SCHEDULE	
16. DISTRIBUTION STATEMENT (of this Report) Approved for public release; distribution unlimited.			
17. DISTRIBUTION STATEMENT (of the abstract entered in Block 20, if different from Report)			
18. SUPPLEMENTARY NOTES			
19. KEY WORDS (Continue on reverse side if necessary and identify by block number) Spacecraft charging Environmental modeling Plasma interactions			
20. ABSTRACT (Continue on reverse side if necessary and identify by block number) Although the role of the environment in generating spacecraft potential variations at geosynchronous orbit is well documented, variations in the ambient environment itself have not been well-defined. Similarly, no studies of the environment have attempted an analytic formulation of the various parameters needed to model the spacecraft charging phenomenon. This paper describes the parameters needed to formulate such a model and outlines a systematic procedure for constructing a simple analytic model that includes			

DDC
APR 25 1980
F

DD FORM 1 JAN 73 1473 EDITION OF 1 NOV 68 IS OBSOLETE

Unclassified

SECURITY CLASSIFICATION OF THIS PAGE (When Data Entered)

409 518 JOB

Unclassified

SECURITY CLASSIFICATION OF THIS PAGE(When Data Entered)

20. Abstract (Continued)

the effects of local time and geomagnetic activity. Observational data from the ATS-5 satellite are analyzed using this procedure to give a preliminary analytic description of the geosynchronous environment in the form of a FORTRAN program.

Unclassified

SECURITY CLASSIFICATION OF THIS PAGE(When Data Entered)

Preface

The author wishes to thank C. Pike, Maj. J. Durrett, Dr. P. Rothwell, Dr. A. Rubin, C. Purvis, Dr. W. Burke, Dr. F. Rich, Dr. S. DeForest, M. Massarro, and G. Inouye for their careful review and comments on the manuscript. Special appreciation is expressed to Dr. S. DeForest of the University of California at San Diego, for providing the data and to R. McInerney of the Air Force Geophysics Laboratory, Analysis and Simulation Branch, for preparing the data for analysis. Useful discussions and data interchange were also provided by Dr. A. Konradi of Johnson Spaceflight Center and Dr. S.-Y. Su.

ADDRESS ONLY

HHS
HHS
HHS

Wife Section ☒
B.H. Section ☐

EDUCATION HISTORY ADULT CODES

SPECIAL

A

Contents

1. INTRODUCTION	7
2. PLASMA CHARACTERIZATION	8
3. METHOD OF ANALYSIS	14
4. DATA BASE	17
5. RESULTS	18
6. MODEL USAGE	28
7. CONCLUSION	34
REFERENCES	35
APPENDIX A: Calculation of Moments	37
APPENDIX B: Calculation of the 2 Maxwellian Distribution	39
APPENDIX C: FORTRAN Listing of Environmental Model	43

Illustrations

1. Actual Maxwellian Fit and 2 Maxwellian Fit Distribution Functions for 30 Sept 1969; (a) Electrons, and (b) Ions	13
2. Example of a Geomagnetic Storm Showing the SSC (storm sudden commencement) and the Resulting Magnetic Variations at the Earth's Surface (Akasofu and Chapman, 1972)	15

Illustrations

3. Histogram of the Occurrence Frequency of A_p , the Daily Sum of a_p , for the Years 1932 through 1975	30
4. Maxwellian and 2 Maxwellian Electron Distribution Functions Predicted by the Model for A_p of 120 and a Local Time of 0130	32
5. Maxwellian and 2 Maxwellian Ion Distribution Functions Predicted by the Model for A_p of 120 and a Local Time of 0130	32
6. Local Time Plot of the Values of the Four Electron Moments Predicted by the Model for A_p of 120	33
7. Local Time Plot of the Values of the Four Ion Moments Predicted by the Model for A_p of 120	33

Tables

1. Geomagnetic Activity for Days Analyzed	18
2. Default Values and Standard Deviations for Model	19
3. Electron Density $\times 100$ (number/cm ³)	20
4. Ion Density $\times 100$ (number/cm ³)	20
5. Electron Pressure $\times 10^{10}$ (dynes/cm ²)	20
6. Ion Pressure $\times 10^{10}$ (dynes/cm ²)	21
7. Electron Energy Flux $\times 100$ (erg/cm ² sec-sr)	21
8. Ion Energy Flux $\times 100$ (erg/cm ² sec-sr)	21
9. Electron Number Flux $\times 10^{-6}$ (number/cm ² sec-sr)	22
10. Ion Number Flux $\times 10^{-6}$ (number/cm ² sec-sr)	22
11. Electron Mean Energy (eV)	22
12. Ion Mean Energy (eV)	23
13. Electron Current $\times 10^4$ (n amps/cm ²)	23
14. Ion Current $\times 10^4$ (n amps/cm ²)	23
15. Electron Density 1 $\times 100$ (number/cm ³)	24
16. Ion Density 1 $\times 100$ (number/cm ³)	24
17. Electron Temperature 1 (eV)	24
18. Ion Temperature 1 (eV)	25
19. Electron Density 2 $\times 100$ (number/cm ³)	25
20. Ion Density 2 $\times 100$ (number/cm ³)	25
21. Electron Temperature 2 (eV)	26
22. Ion Temperature 2 (eV)	26

Modeling of the Geosynchronous Orbit Plasma Environment-Part I

1. INTRODUCTION

Although the role of the environment in generating spacecraft potential variations at geosynchronous orbit is well documented,^{1-4*} variations in the ambient environment itself have not been well-defined. Several studies have been made of the geosynchronous environment,⁵⁻⁸ but none have attempted an analytic formulation of the various parameters needed by the user community in modeling the spacecraft charging phenomenon. This initial paper describes the basic set of parameters required to formulate such a model of the ambient plasma environment and outlines a systematic procedure for constructing a simple analytic model that includes the effects of local time and geomagnetic activity. Observational data from the ATS-5 satellite are analyzed using this procedure to give a preliminary analytic description of the geosynchronous environment in the form of a FORTRAN program. Although not intended as a detailed description of the environment, the model is used in evaluating local time variations of the plasma following a plasma injection event at geosynchronous orbit (the condition most likely to foster charging).

(Received for publication 13 December 1977)

*Due to the number of references to be included as footnotes on this page, the reader is referred to the list of references, page 35.

2. PLASMA CHARACTERIZATION

The first step in constructing any model is the determination of the critical parameters necessary for description of the phenomenon. In plasma physics, classical studies have shown that to describe a plasma completely, the electric field, magnetic field, and particle distribution functions must be known. Several models of the magnetospheric electric and magnetic fields exist in the open literature so they will not be discussed here. This paper will concentrate instead on the so-called plasma distribution function - its definition, its use, and its measurement.

What is the plasma distribution function? Although in general a complex concept, the distribution function is, stripped of its physical and mathematical niceties, a function which describes how many particles exist within a tiny volume of space with a velocity in a certain direction. Turning briefly to the mathematical details, one notes that F , the distribution function, is given by:

$$F(X, Y, Z, V_X, V_Y, V_Z) \quad (1)$$

such that

$$F(X, Y, Z, V_X, V_Y, V_Z) dx dy dz dv_x dv_y dv_z$$

is the number of particles in the velocity space

$$dv_x dv_y dv_z \text{ and spatial volume } dx dy dz$$

where

$$X, Y, Z = \text{spatial coordinates}$$

and

$$V_x, V_y, V_z = \text{velocity components.}$$

If F is integrated over all velocities and positions within a given volume, the total number of particles in that volume is obtained (the analysis presented in this paper assumes a collisionless plasma with no particle sources or sinks).

For the purposes of this study, the plasma will be considered to be isotropic; that is, there are just as many particles traveling in direction X as in direction Y or Z . This simplifies the analysis greatly. (Only future study will reveal just

how good or bad such an assumption is and this factor should be kept in mind in the following.) Changing to spherical coordinates, one notes:

$$\begin{aligned} F(X, Y, Z, V_x, V_y, V_z) dx dy dz dv_x dv_y dv_z \\ = f(X, Y, Z, v) dx dy dz v^2 \sin \theta_v d\theta_v d\phi_v dv \\ = f(X, Y, Z, v) dx dy dz (4\pi v^2 dv) \end{aligned} \quad (2)$$

where

$$v = (v_x^2 + v_y^2 + v_z^2)^{1/2}$$

θ_v, ϕ_v = angular coordinates of the velocity vector

f = isotropic distribution function

And we have integrated over θ_v and ϕ_v :

$$\int_0^{2\pi} d\phi_v \int_0^\pi \sin \theta_v d\theta_v = 4\pi \quad (3)$$

A commonly encountered distribution function is the so-called Maxwellian distribution:

$$f(v_i) = n_i \left(\frac{m_i}{2\pi k T_i} \right)^{3/2} e^{-m_i v_i^2 / 2k T_i} \quad (4)$$

where

n_i = number density of species i

m_i = mass of species i

T_i = temperature of species i

v_i = velocity of i species

k = Boltzmann constant

f = distribution function in sec^3/cm^3

Although most plasma distributions in space are neither Maxwellian nor isotropic, these assumptions are commonly made in characterizing a plasma, in order to reduce the number of parameters necessary for description. Further, Eq. (4) can be used in the calculation of the first four plasma moments that will generate the model. For a Maxwellian particle distribution, they are:

$$\langle n_i \rangle = 4\pi \int_0^\infty (v^0) f_i v^2 dv = n_i \quad (5)$$

$$\langle NF_i \rangle = \int_0^\infty (v^1) f_i v^2 dv = \frac{n_i}{2\pi} \left(\frac{2kT_i}{\pi m_i} \right)^{1/2} \quad (6)$$

$$\langle P_i \rangle = 4\pi \left(\frac{1}{3} m_i \right) \int_0^\infty (v^2) f_i v^2 dv = n_i kT_i \quad (7)$$

$$\langle EF_i \rangle = \left(\frac{1}{2} m_i \right) \int_0^\infty (v^3) f_i v^2 dv = \frac{m_i n_i}{2} \left(\frac{2kT_i}{\pi m_i} \right)^{3/2} \quad (8)$$

where

$\langle n_i \rangle$ = number density for species i (number/cm³)

$\langle NF_i \rangle$ = number flux for species i (number/cm² sec-sr)

$\langle P_i \rangle$ = pressure for species i (dynes/cm²)*

$\langle EF_i \rangle$ = energy flux for species i (ergs/cm² sec-sr)

The use of moments is similar to expanding a function in a Taylor series. The moments are, in statistical terms, the expectation values of a variable, that is, the average value, the standard deviation, and so on). For a plasma, the moments of the velocity are taken as follows: $\langle v^0 \rangle$, $\langle v^1 \rangle$, $\langle v^2 \rangle$, and $\langle v^3 \rangle$. In Eqs. (5), (6), (7) and (8), these moments have been multiplied by constants to give physically meaningful quantities. For example, the $\langle v^2 \rangle$ moment has been multiplied by 4π and $1/3 m_i$ to give the isotropic pressure, $4\pi \langle 1/3 m_i v^2 \rangle$.

* $\langle P_i \rangle$ is two-thirds of the so-called energy density which is in units of ergs/cm³. The energy density is the total energy per unit volume of the plasma.

The moments, easily derived from the UCSD ATS-5 data (the instrument employed in this study), can be used to derive, a Maxwellian and a "2-Maxwellian" fit to the distribution function, as will be demonstrated.

An interesting and important feature of the four moments is that they (unlike the plasma temperature) can be averaged together to give a physically meaningful average quantity. To prove this, assume a particle distribution is given by f_i . Then the moments for this function are given by

$$\langle M \rangle_i = \int_0^{\infty} M f_i v^2 dv$$

where M is the moment to be found for distribution i . Now assume we want to find $\langle M \rangle$ for a distribution function f where, f is the average of several distribution functions f_i :

$$f = \frac{1}{N} \sum_{i=1}^N f_i$$

Then $\langle M \rangle$ can be defined as:

$$\langle M \rangle = \int_0^{\infty} M f v^2 dv$$

This gives:

$$\begin{aligned} \langle M \rangle &= \int_0^{\infty} M f v^2 dv = \int_0^{\infty} M \left(\frac{1}{N} \sum_{i=1}^N f_i \right) v^2 dv \\ &= \frac{1}{N} \sum_{i=1}^N \left(\int_0^{\infty} M f_i v^2 dv \right) = \frac{1}{N} \sum_{i=1}^N \langle M \rangle_i \end{aligned}$$

Thus groups of the four moments can each be averaged to give a new average set of moments in an entirely consistent fashion. These, in turn, can be used to derive a new, averaged distribution function.

In Appendix A, it is demonstrated that if, instead of Eq. (1), the distribution function is assumed to be the sum of 2 Maxwellians or 2 plasma components for a single species i , then n_{1i} , n_{2i} , T_{1i} , and T_{2i} can be found from Eqs. (5), (6), (7), and (8) such that:

$$f(v) = \left(\frac{m_i}{2\pi k} \right)^{3/2} \left(\frac{n_{1i}}{T_{1i}^{3/2}} e^{-m_i v^2 / 2kT_{1i}} + \frac{n_{2i}}{T_{2i}^{3/2}} e^{-m_i v^2 / 2kT_{2i}} \right) \quad (9)$$

In Figure 1 are plotted actual distribution functions, the Maxwellian fit, and the 2 Maxwellian fit. Neither exactly fits the distribution functions but, of the two approximations, the 2 Maxwellian fit gives a much better representation of the actual distribution function (for most studies of the effects of the ambient environment, a single Maxwellian has been considered adequate — clearly a dubious assumption). In this paper, the parameters necessary to compute both the single Maxwellian and 2 Maxwellian distributions will be derived. Figure 1, however, should be remembered in considering the accuracy of either representation.

The second moment, $\langle NF_i \rangle$, may be utilized in the calculation of another important quantity, the current per unit area to the spacecraft. As the charge striking a unit area of the spacecraft per unit time is of concern, the vector velocity \vec{v}_i relative to the unit normal \vec{n} to the surface must be taken into account. Also, only particles entering one half of the sphere (that is, particles reaching the satellite surface from one side only) are considered. Thus:

$$\begin{aligned} J_i &= q_i \int \vec{v}_i \cdot \vec{n} f d^3 v \\ &= q_i \int_0^{\pi/2} \sin \theta_v \cos \theta_v d\theta_v \int_0^{2\pi} d\phi_v \int_0^\infty f v^3 dv \\ &= \frac{q_i n_i}{2} \left(\frac{2kT_i}{\pi m_i} \right)^{1/2} = q_i \pi \langle NF_i \rangle \end{aligned} \quad (10)$$

where

q_i = charge on species (coulombs)

J_i = current per unit area (amps/cm²).

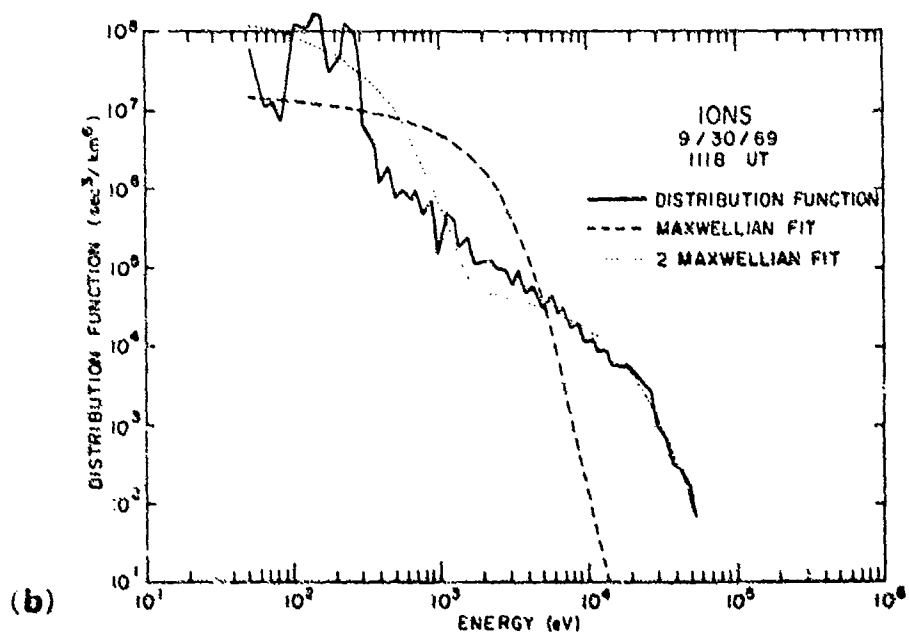
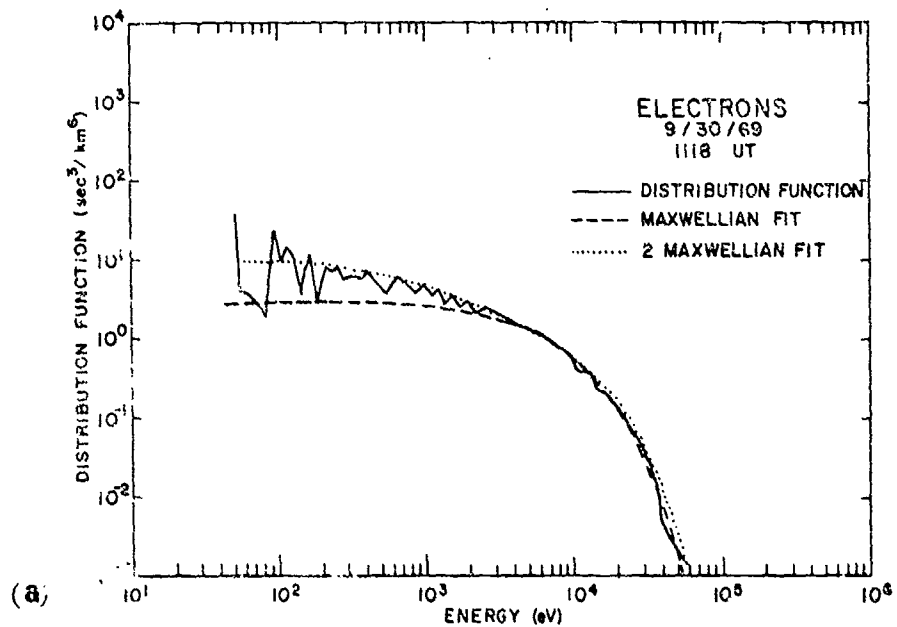


Figure 1. Actual Maxwellian Fit and 2 Maxwellian Fit Distribution Functions for 30 Sept 1969; (a) Electrons, and (b) Ions

Another quantity of general usage is the mean energy. The mean energy, $\langle E_i \rangle$ (that is, the average energy per particle), for a Maxwellian distribution is defined as the ratio of the energy density to the number density (where $\langle P_i \rangle$ is two-thirds of the energy density):

$$\langle E_i \rangle = \frac{3}{2} \langle P_i \rangle / \langle n_i \rangle = \frac{3}{2} kT_i \quad (11)$$

where kT_i , the quantity used in defining the Maxwellian distribution, can be obtained from $\langle E_i \rangle$ by means of this relation.

The distribution function (approximated either by a Maxwellian or, better, 2 Maxwellian fit), the mean energy, and current are the three quantities most often required by programs designed to calculate spacecraft-plasma interactions. Thus, given the four moments and Eqs. (4), (9), (10), and (11), a description of the plasma environment can be derived which meets the majority of the user community's needs.

3. METHOD OF ANALYSIS

In the preceding section, the parameters necessary to define the ambient plasma were described. All exhibit large temporal and spatial variations at geosynchronous orbit, making their accurate determination quite difficult. In fact, it is this extreme variation, particularly during geomagnetic storms, that has prevented analytic models from being generated. The method to be outlined is, as a result, a first-order approximation. Its usefulness can be determined only in retrospect by how well it predicts conditions at geosynchronous orbit. We can, however, describe the characteristics of a meaningful model and build those explicitly into the analysis process.

What characteristics must a model of the geosynchronous environment possess? In particular, how can the observed temporal and spatial variations be accounted for? The scale of the variations give important clues to the answer. First, changes in geomagnetic activity correlate with the largest temporal variations in the plasma. Secondly, spatial variations at geosynchronous orbit translate into local time (or position relative to the sun) variations. Thus, the two important variations are geomagnetic activity and local time.

Geomagnetic activity has been defined historically in terms of geomagnetic storms at the earth's surface.⁹ These storms appear as initially small increases in the earth's horizontal magnetic field amplitude (~10 - 100 γ,

9. Rostoker, G. (1972) Geomagnetic indices. Rev. Geophys. 10(No. 4):935.

where a γ is 10^{-5} of a gauss - the earth's field is ~ 0.3 gauss) followed by a rapid $\sim 1000 \gamma$ decrease. This decrease may last a day or more after which the field slowly (\sim week) recovers to its quiet value. Such events are believed to be the result of a compression of the earth's magnetic field by the solar wind and are generally accompanied by auroral activity, ionospheric perturbations, particle fluxes at geosynchronous orbit, and so on. A typical magnetic record is shown in Figure 2.

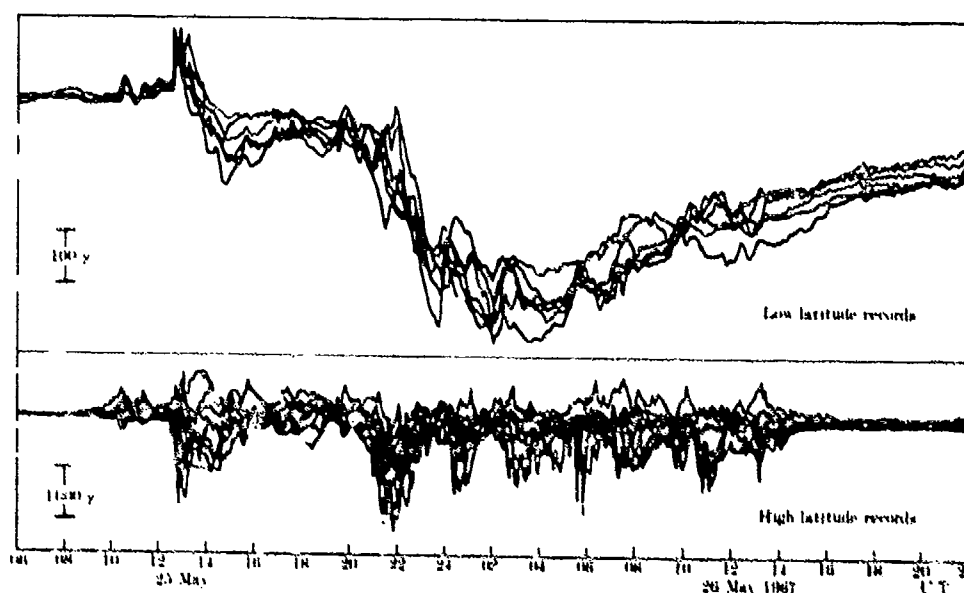


Figure 2. Example of a Geomagnetic Storm Showing the SSC (storm sudden commencement) and the Resulting Magnetic Variations at the Earth's Surface (Akasofu and Chapman, 1972)

Traditionally, the level of world-wide geomagnetic activity as represented by fluctuations in the earth's magnetic field has been defined by the 3 hour K_p index which goes from 0 to 9 in steps of $1/3$. This is a quasi-logarithmic quantity which is supposed to represent the positive and negative deviation of an "average" magnetometer at mid-latitudes. The a_p index is directly calculated from the K_p index and, when multiplied by 2γ 's is supposed to give the magnetic deviation in γ 's.⁹ These two quantities, due to the localized nature of most geomagnetic activity, are underestimates of actual geomagnetic activity. They are, however,

the only quantities currently available. In this study, A_p , the daily sum of a_p , will be employed as the index of geomagnetic activity.*

The determination of how the distribution function changes in local time and with A_p is a significantly different problem from determining average conditions or extreme values. This is particularly true in a study of charge buildup for the proper relationship between A_p and local time relative to the sun of the satellite and the interrelationship between parameters must be preserved simultaneously. Finally, in order to make the model of general utility, it should be expressible in an analytical form. To fulfill these requirements, a multiple linear regression analysis was carried out.

In multiple regression, the coefficients of a simple analytic expression are adjusted so that the deviations between the observed and predicted values as described by the chi-squared statistic are minimized. For this initial study, a linear relation in daily A_p and a diurnal and semidiurnal variation in local time t were selected. That is, a collection of observations varying in local time and A_p of a given moment were fit using the following equation:

$$M(t, A_p) = (a_0 + a_1 A_p)(b_0 + b_1 \cos \left[\frac{\pi}{12} (t + t_1) + b_2 \cos \left(\frac{\pi}{6} (t + t_2) \right) \right]) \quad (12)$$

where: $M(t, A_p)$ = predicted value of the moment M at local time t and for the daily geomagnetic activity index A_p , and $a_0, a_1, b_0, b_1, b_2, t_1, t_2$ = coefficients determined by the regression. Using a multiple regression program, from Bevington,¹⁰ we note that $a_0, a_1, b_0, b_1, b_2, t_1$, and t_2 were determined for each set of moments, A_p , and t . The standard deviation for each point was assumed to be the standard deviation of each set of moments for analysis purposes.

In summary, the plasma environment at geosynchronous orbit varies with geomagnetic activity and local time (that is, the position of the satellite relative to the sun). To preserve this relationship, each parameter is fit, using multiple linear regression, to a simple function in A_p and local time. Each parameter, predicted for the same value of A_p and local time, can then be combined to give the distribution function and other parameters of interest. A FORTRAN listing of the resulting model is given in Appendix A.

10. Bevington, P. R. (1969) Data Reduction and Error Analysis for the Physical Sciences. McGraw-Hill, New York.

* A_p was employed in lieu of a_p , as the spread in a_p in the data base was inadequate in local time for meaningful comparisons. The use of A_p also allows the analytic expression to include the observation that particle injections at geosynchronous orbit produce effects lasting up to 24 hours.

4. DATA BASE

To test the method just described, measurements made by the University of California at San Diego (UCSD) plasma experiment on ATS-5 were analyzed. In August 1969, ATS-5 was launched into geosynchronous orbit ($6.6 R_E$) near $105^\circ W$. The satellite spin period is 0.79 sec and the spin axis is aligned with that of the earth's. The UCSD instrument consists of four cylindrical plate spectrometers: two pairs of electron and positive ion detectors directed parallel and perpendicular to the spin axis. Three simultaneous measurements, 0.26 sec long, can be taken every 0.32 sec. A complete spectrum of 64 steps of energy channels (two are background, the others are each 112 percent of the previous channel starting at 51.6 eV and ending at 51.6 keV) can be taken in 20.48 sec. Other modes are possible, but for this study only two to four minute averages of the four moments of the distribution function are studied. A more detailed description of the calculation of the four moments from the UCSD data is given in Appendix A.

As the primary purpose of this paper is to outline a procedure for obtaining an analytic formulation of the geosynchronous plasma useful in studying charging effects, we do not use a large data set nor are the days selected at random (see the following). Ten days of hourly measurements were chosen which covered a wide range of geomagnetic activity. Data gaps and other singularities were ignored and interpolated values employed (even so, this involved only about 8 of the 240 observations). Table 1 lists the ten days chosen and the corresponding 3-hour a_p and daily A_p values (see Rostoker,⁹ for a review of geomagnetic indices). Initially 250 sets of moments were selected (one set every hour on the half-hour plus the values at plasma injection, if clearly identifiable). The plasma components perpendicular and parallel to the satellite spin axis were averaged together, assuming equal weights. Finally, to facilitate a comparison with the 3-hour a_p index, 3-hour averages were taken. It was this data base of 80 values per moment which was analyzed.

The data base was not selected at random to avoid errors in the local time variations which are affected by single injection events. As discussed in DeForest and McIlwain⁵ or Garrett et al.,⁴ an injection event is the sudden appearance of hot, plasma sheet plasma near local midnight at geosynchronous orbit. Unfortunately, these events are by their very nature random in occurrence. Such events cause order of magnitude changes in the plasma conditions at geosynchronous orbit and tend to skew any gross averages of the geosynchronous environment.

* The electron data for 1972, by which time these detectors had degraded, were corrected using a factor of 48 for the parallel detector and 0 for the detector perpendicular to the spin axis.

Table 1. Geomagnetic Activity for Days Analyzed

Year	Day	Hourly AP								Daily AP
1972	217	67	236	132	27	56	27	111	400	1056
1970	348	22	80	236	48	32	15	32	56	521
1972	223	9	6	12	18	32	27	15	27	146
1969	326	15	18	12	7	5	5	12	6	80
1970	273	6	18	18	5	7	6	4	9	73
1970	272	3	5	6	5	2	3	2	12	38
1969	299	3	4	9	3	4	2	5	3	33
1970	25	4	3	2	0	2	2	3	4	20
1971	87	5	2	0	0	2	2	4	3	18
1970	345	0	2	3	3	2	0	2	2	14

As the purpose of this analysis is to model the time-history of a charging event, we have selected days exhibiting single injection events near satellite midnight, for the lower levels of geomagnetic activity. Such steps were based on the observation that spacecraft charging has been found to occur primarily in conjunction with individual plasma injections near midnight. This bias should be considered when evaluating the generality of the model.

5. RESULTS

A variety of parameters and combinations of parameters were calculated for this study. Considering the sparseness of the data base, we have limited the study to a formulation of the four moments in terms of linear regression-derived analytic expressions.^{*} The currents and the parameters necessary for a Maxwellian and a 2 Maxwellian fit to the distribution function are computed from these predicted quantities. As a result of the simplicity of the fitted function (in particular the assumed linearity of A_p) and the paucity of data, some negative values result for the predicted values. As these, in turn, result in fictitious values for the derived quantities, in the FORTRAN formulation of the problem, these values have been corrected by estimates (see Table 2). With this caveat

* The average energy was calculated from the data and was derived from the fitted values. The latter values are used in this preliminary model to preserve the internal consistency of the model, since the differences between the values so derived are within the accuracy of the model.

Table 2. Default Values and Standard Deviations for Model

Variable	Units	Electrons		Ions	
		Std.	Dev./Default	Std.	Dev./Default
Density	no#/cm ³	0.67	0.02	0.55	0.33
Pressure	dynes/cm ²	2.6×10^{-9}	4×10^{-11}	4.9×10^{-9}	4×10^{-9}
Energy flux	erg/(cm ² -sec-sr)	2.1	0.08	0.13	0.09
Number flux	no#/(cm ² sec-sr)	1.4×10^8	4×10^6	4×10^6	3×10^6
Mean Energy	eV	(1600)	1000	(1820)	
Current	nAmps/cm ²	0.07	0.002	0.002	0.0015
N1	no#/cm ³		2		
N2	no#/cm ³		0.04		
T1	eV		250		
T2	eV		20000		

in mind, the model predictions will be discussed and, where possible, compared with other observations.

Tables 3 through 22 list, by parameter, the values predicted by the model (see FORTRAN listing in Appendices). The parameters are given as a function of the A_p values corresponding to average daily values of K_p of 0, 1, 2, 3, 4, 5, 6, 7, 8, and 9. As the data set of A_p values includes only values as high as 1056 (that is, $K_p = 7$), the values for 1656 and 3200 should be treated as extrapolations. For each of the four moments and for the current, the standard deviation associated with the fit to the actual data is given. This is indicative of the error that should be assigned each predicted value. As would be expected for the small data set employed in this study, the predicted errors are a large fraction of the model values. Also, the environment actually exhibits large variations such as these.

In consideration of the errors associated with the four moments, it is not justified to draw more than a few generalized conclusions from the predictions of this preliminary model. In general, the ranges of the four moments well approximate those given by DeForest and Mellwain⁵ in their Table 1 if their "maximum" values are taken as corresponding to an A_p of ~ 1056 (average K_p of 7), their "typical" values as corresponding to A_p of ~ 120 (average K_p of 3), and "minimum" to an A_p of ~ 0 (average K_p of 0). The agreement is excellent for the ions as to actual

Table 3. Electron Density $\times 100$ (number/cm³)

DAILY AP	1.5	4.5	7.5	LOCAL TIME	13.5	16.5	19.5	AVERAGE
3200	1418.7	1329.6	1592.1	10.5	1334.4	892.9	1049.6	1400.0
1556	782.8	735.6	805.7	1001.5	751.8	463.1	539.4	743.8
1056	534.6	585.0	563.5	645.2	486.5	295.1	341.1	487.7
640	367.1	763.1	373.4	396.3	302.6	189.3	203.6	310.7
384	277.5	243.5	241.8	246.3	189.5	102.1	119.0	201.8
216	188.2	178.1	154.1	146.5	115.7	62.3	63.5	130.3
128	144.2	140.2	104.5	89.5	72.7	35.6	31.8	89.4
56	122.3	115.8	71.4	51.6	44.4	17.8	10.6	62.2
32	112.4	106.4	59.0	37.3	33.5	11.1	2.7	52.0
0	99.2	94.0	62.6	18.3	19.7	2.2	2.0	39.6

Table 4. Ion Density $\times 100$ (number/cm³)

DAILY AP	1.5	4.5	7.5	LOCAL TIME	13.5	16.5	19.5	AVERAGE
3200	444.1	317.8	431.0	10.5	440.8	602.1	733.9	764.1
1556	398.4	338.0	490.0	601.3	477.0	345.9	414.5	443.0
1056	231.8	260.7	354.0	421.2	335.8	246.3	290.4	340.2
640	223.5	207.1	261.0	296.3	237.8	177.2	204.3	231.6
384	181.4	174.1	203.5	218.4	177.6	134.7	151.3	178.4
216	153.8	152.5	165.4	169.0	139.0	103.6	116.6	143.5
128	132.0	140.1	143.4	140.1	115.4	90.8	96.7	123.5
56	127.5	141.9	123.3	120.9	100.4	91.2	93.5	110.2
32	123.6	128.8	123.9	113.7	94.7	75.2	78.5	105.2
0	118.3	124.6	115.7	104.1	87.2	71.9	71.9	98.5

Table 5. Electron Pressure $\times 1010$ (dynes/cm²)

DAILY AP	1.5	4.5	7.5	LOCAL TIME	13.5	16.5	19.5	AVERAGE
3200	600.2	423.8	515.2	10.5	474.1	292.7	242.8	408.1
1556	216.1	223.3	270.5	585.6	244.0	145.0	124.0	213.7
1056	144.6	154.0	175.5	191.3	154.6	92.1	72.9	130.1
640	95.0	101.8	103.5	114.6	92.7	55.1	45.6	85.8
384	64.5	69.7	63.0	67.7	54.5	32.3	26.1	53.5
216	44.5	68.6	42.4	36.6	29.5	17.4	13.2	32.4
128	33.1	36.6	27.1	19.1	15.2	8.8	5.8	20.3
56	25.4	28.5	17.0	7.3	5.6	3.2	.9	12.2
32	22.6	25.5	13.2	2.9	2.1	1.0	.4	9.4
0	18.5	21.5	9.1	.6	.4	.4	.4	6.8

Table 6. Ion Pressure X 10¹⁰ (dynes/cm²)

DAILY AP	LOCAL TIME	13.5	15.5	19.5	22.5	AVERAGE
3280	1.5	4.5	7.5	10.5	13.5	15.5
1656	642.3	573.8	617.9	702.2	419.4	486.1
1056	462.2	338.5	453.3	393.1	247.8	127.4
	342.3	247.4	250.5	273.0	181.1	103.3
	245.3	187.7	173.2	189.7	174.9	91.7
344	185.7	144.7	135.4	138.5	106.4	82.7
216	146.5	119.1	105.6	104.3	87.8	75.8
128	126.1	104.5	91.1	85.6	77.1	73.4
56	109.2	94.7	79.2	72.8	70.0	71.1
32	103.6	81.0	75.0	68.8	67.3	70.3
0	96.1	85.2	69.6	61.6	63.6	69.2
						77.9
						90.4
						76.8

Table 7. Electron Energy Flux X 100 (erg/cm² sec-sr)

DAILY AP	LOCAL TIME	13.5	16.5	19.5	22.5	AVERAGE
3280	1.5	4.5	7.5	10.5	13.5	16.5
1656	2498.8	2351.2	1496.0	4895.3	4632.4	2820.5
1056	1177.5	872.3	1204.5	2524.8	2375.0	1447.7
640	510.2	585.4	753.8	964.9	1497.8	914.2
344	352.1	408.4	486.2	571.8	889.6	544.4
216	246.4	292.9	305.7	318.9	515.3	313.8
128	189.1	226.2	204.1	166.5	269.6	167.4
56	149.6	182.6	135.5	68.3	35.7	25.1
32	134.8	164.0	113.0	31.4	8.0	3.0
0	115.0	144.0	75.8	8.0	8.0	8.0
						14.7
						58.9
						41.6
						51.0

Table 8. Ion Energy Flux X 100 (erg/cm² sec-sr)

DAILY AP	LOCAL TIME	13.5	16.5	19.5	22.5	AVERAGE
3280	1.5	4.5	7.5	10.5	13.5	16.5
1656	223.0	134.7	123.2	155.4	94.9	32.9
1056	126.0	80.4	73.1	67.3	56.9	23.5
640	88.3	58.5	54.9	61.7	42.1	20.6
344	62.2	43.4	39.4	43.5	31.9	20.6
216	46.1	34.8	33.5	32.3	25.6	13.3
128	35.6	24.0	24.6	25.0	21.4	18.5
56	29.5	24.5	21.2	20.8	19.1	13.1
32	25.5	22.1	13.0	14.0	17.5	20.8
0	24.0	21.2	16.1	16.9	16.9	17.6
	22.0	20.1	17.6	15.5	16.1	17.5
						19.2
						21.3
						23.4
						19.8
						21.6

Table 9. Electron Number Flux $\times 10^{-6}$ (number/cm² sec-ar)

DAILY AD	1.5	4.5	7.5	LOCAL TIME	13.5	16.5	19.5	AVERAGE
1200	3841.1	1076.6	1155.7	1113.3	2175.9	1434.7	1784.0	2639.2
1356	1045.5	1665.0	1761.8	1714.3	1236.7	773.8	910.3	1308.5
1556	1101.1	1115.5	1142.4	1042.8	794.0	433.6	570.7	902.5
640	727.1	736.2	712.9	662.0	467.0	293.4	335.3	565.6
884	495.7	502.1	448.6	396.9	298.1	175.9	198.5	358.2
216	343.3	340.6	275.2	222.9	174.2	101.4	95.4	222.1
420	252.1	260.8	176.1	123.5	103.3	55.6	41.1	144.4
56	199.2	202.3	110.0	57.2	56.1	25.7	4.9	92.5
32	127.5	180.4	85.3	32.3	38.4	15.5	4.0	74.7
0	148.6	151.1	52.2	4.0	14.6	4.0	4.0	37.9
								52.1

Table 10. Ion Number Flux $\times 10^{-6}$ (number/cm² sec-ar)

DAILY AD	1.5	4.5	7.5	LOCAL TIME	13.5	16.5	19.5	AVERAGE
1200	61.7	43.8	60.8	70.0	45.3	24.1	46.4	51.5
1356	36.3	25.9	34.4	38.6	25.8	14.9	25.8	30.7
1556	26.5	21.1	24.1	26.5	18.2	11.3	18.5	21.8
640	19.3	15.0	17.0	15.0	12.9	5.0	13.5	15.7
884	14.0	12.8	12.6	12.8	9.7	7.3	10.4	11.9
216	12.0	10.3	8.7	9.4	7.6	6.3	6.4	9.6
420	11.1	8.1	8.1	7.5	6.4	5.7	7.2	8.0
56	9.2	8.3	7.0	6.2	5.6	5.3	6.5	7.1
32	8.8	8.0	6.6	5.7	5.3	5.2	6.2	6.7
0	8.3	7.6	6.0	5.1	4.9	5.0	5.8	6.2

Table 11. Electron Mean Energy (eV)

DAILY AD	1.5	4.5	7.5	LOCAL TIME	13.5	16.5	19.5	AVERAGE
1200	2540.2	2955.4	2841.4	2858.4	3093.8	2963.3	2165.3	2714.9
1356	9587.8	2385.4	2817.4	2419.7	3038.4	2933.7	2152.1	2678.8
1556	2532.2	2854.8	2792.6	2725.1	2975.0	2902.6	2136.3	2638.9
640	2450.3	2777.1	2745.9	2697.6	2865.7	2859.5	2107.3	2573.1
884	2145.6	2529.1	2678.7	2532.0	2692.8	2722.7	2056.2	2474.7
216	2213.2	2555.1	2571.8	2348.4	2395.1	2603.7	1948.5	2314.0
420	2082.1	2432.5	2431.8	1996.9	1951.8	2324.5	1718.2	2079.9
56	1947.6	2306.4	2228.4	1370.9	1185.9	1659.4	1000.0	1648.5
32	1888.4	2244.4	2891.7	731.6	1000.0	1000.0	1000.0	1407.8
0	1771.1	2145.1	1791.8	1000.0	1000.0	1000.0	1000.0	1335.4

Table 12. Ion Mean Energy (eV)

DATE AP	LOCAL TIME					AVERAGE				
	1.5	6.5	7.5	12.5	13.5	16.5	19.5	22.5		
1280	12240.5	1001.9	6901.1	6172.0	4670.5	2827.2	6198.9	9971.0	7372.3	
1656	11562.3	9373.7	6743.0	6116.3	4652.3	7445.7	6529.7	9876.2	7314.8	
1056	18988.6	8970.0	6609.4	6066.8	4048.9	4040.2	6853.7	9785.0	7281.9	
542	10276.3	8701.9	6427.6	5993.4	5308.3	643.5	7310.1	9660.0	7265.1	
384	9578.5	7777.6	6232.5	5986.4	5610.2	5747.3	7849.1	9517.1	7272.4	
216	8913.5	7310.3	6030.4	5807.1	5951.5	6731.6	8468.9	9350.5	7321.5	
120	8414.2	6976.4	5867.1	5717.8	6251.6	7565.4	9023.1	9221.8	7379.9	
56	8012.7	6722.6	5727.9	5634.7	6526.7	8305.3	9539.0	9098.6	7446.0	
32	7344.5	6618.2	5667.4	5598.3	6652.5	8636.0	9777.4	9043.0	7479.4	
0	7602.8	6470.9	5577.9	5536.9	6845.5	9134.7	10146.4	8958.4	7534.2	

Table 13. Electron Current $\times 10^4$ (n amps/cm²)

DATE AP	LOCAL TIME					AVERAGE				
	1.5	4.5	7.5	10.5	13.5	16.5	19.5	22.5		
1280	15286.3	15461.0	15867.7	16654.6	11942.7	7513.1	8967.2	13432.4	13266.0	
1656	6271.1	6359.1	6853.7	6616.8	4216.2	3883.4	4575.4	7043.2	6979.6	
1056	5945.0	5612.0	5742.2	5493.2	3990.9	2431.3	2858.8	4560.3	4536.7	
648	3654.8	3700.4	3583.5	3727.6	2448.0	1504.9	1685.5	2038.9	2843.0	
384	2491.7	2524.1	2255.1	1984.2	1498.5	904.1	957.3	1779.5	1800.7	
216	1728.3	1752.1	1383.4	1120.3	675.4	509.8	479.5	1084.3	1116.6	
120	1202.2	1311.8	885.2	620.6	519.3	284.5	206.4	587.1	725.8	
56	1001.4	1016.9	553.1	287.4	782.8	134.3	24.4	422.2	465.2	
32	802.3	906.6	424.6	162.5	193.0	71.0	20.1	322.9	375.5	
0	746.3	759.5	262.5	20.1	74.3	28.1	20.1	190.5	261.8	

Table 14. Ion Current $\times 10^4$ (n amps/cm²)

DATE AP	LOCAL TIME					AVERAGE				
	1.5	4.5	7.5	10.5	13.5	16.5	19.5	22.5		
1280	320.0	245.1	305.0	351.6	227.5	121.1	223.0	358.5	269.1	
1656	185.7	145.1	172.8	194.2	129.5	76.8	129.5	203.3	154.4	
1056	133.4	106.3	121.1	133.1	91.4	55.8	93.1	143.0	109.8	
648	97.2	79.4	85.3	90.7	65.0	44.3	67.9	101.2	78.9	
384	75.0	62.0	63.3	64.6	48.8	35.6	52.4	75.4	59.9	
216	60.3	52.0	49.8	47.4	38.1	31.6	42.2	58.5	47.4	
120	52.0	45.7	43.5	37.7	32.8	29.7	36.4	48.9	40.2	
56	46.4	41.6	35.0	31.1	27.9	26.8	32.5	42.5	35.5	
32	44.3	40.0	33.0	28.7	26.4	25.0	31.1	40.0	33.7	
0	41.6	38.0	33.2	25.4	24.4	25.1	29.2	36.8	31.3	

Table 15. Electron Density 1×100 (number/cm³)

DAILY AP	LOCAL TIME	LOCAL TIME	LOCAL TIME	AVERAGE
1200	1.5	6.5	7.5	19.5
1556	1247.5	4310.9	1228.5	15.5
1856	653.9	701.6	1477.1	753.0
2056	122.8	459.2	776.5	1158.2
540	278.3	290.0	632.1	396.2
814	192.4	131.8	277.5	252.9
216	140.1	137.2	182.4	154.9
128	113.5	124.2	113.9	177.8
56	96.9	84.7	84.0	106.0
22	80.4	70.5	70.9	58.2
0	61.1	51.4	49.0	30.2
		38.3	32.0	17.4
		18.3	13.6	11.1
			19.7	2.2
				2.0

Table 16. Ion Density 1×100 (number/cm³)

DAILY AP	LOCAL TIME	LOCAL TIME	LOCAL TIME	AVERAGE
1200	1.5	6.5	7.5	19.5
1556	1247.5	4310.9	1228.5	15.5
1856	653.9	701.6	1477.1	753.0
2056	122.8	459.2	776.5	1158.2
540	278.3	290.0	632.1	396.2
814	192.4	131.8	277.5	252.9
216	140.1	137.2	182.4	154.9
128	113.5	124.2	113.9	106.0
56	96.9	84.7	84.0	58.2
22	80.4	70.5	70.9	30.2
0	61.1	51.4	49.0	17.4
		38.3	32.0	11.1
		18.3	13.6	2.2
			19.7	2.0

Table 17. Electron Temperature 1 (eV)

DAILY AP	LOCAL TIME	LOCAL TIME	LOCAL TIME	AVERAGE
1200	1.5	6.5	7.5	19.5
1556	1247.5	4310.9	1228.5	15.5
1856	653.9	701.6	1477.1	753.0
2056	122.8	459.2	776.5	1158.2
540	278.3	290.0	632.1	396.2
814	192.4	131.8	277.5	252.9
216	140.1	137.2	182.4	154.9
128	113.5	124.2	113.9	106.0
56	96.9	84.7	84.0	58.2
22	80.4	70.5	70.9	30.2
0	61.1	51.4	49.0	17.4
		38.3	32.0	11.1
		18.3	13.6	2.2
			19.7	2.0

Table 18. Ion Temperature 1 (eV)

DAILY AD	LOCAL TIME	7.5	10.5	13.5	16.5	19.5	AVERAGE
1280	1.5	6.5	7.5	10.5	13.5	16.5	22.5
1556	158.3	257.6	187.4	370.8	414.5	473.3	216.6
1656	113.7	168.5	155.5	305.9	346.2	44.0	57.3
1856	49.0	121.4	133.0	248.2	270.2	29.6	165.9
540	64.3	87.3	113.1	186.6	184.3	63.7	130.6
294	45.6	65.8	83.6	129.2	103.4	27.6	92.3
216	30.4	51.9	72.2	83.8	51.5	3.7	60.5
120	28.7	44.2	68.3	55.0	20.1	1.2	37.4
56	13.9	39.2	51.4	35.5	4.6	15.2	26.7
32	11.4	37.2	47.8	28.4	1.2	27.1	24.4
0	8.0	34.9	42.6	19.4	.2	52.2	25.6
						78.3	30.2

Table 18. Electron Density 2×100 (number/cm³)

DAILY AD	LOCAL TIME	7.5	10.5	13.5	16.5	19.5	AVERAGE
1280	1.5	4.5	7.5	10.5	13.5	16.5	22.5
1556	171.2	24.7	468.5	441.1	276.2	114.0	820.7
1656	123.7	37.0	243.8	225.0	141.6	63.9	277.5
1856	106.6	45.0	154.4	144.0	80.3	47.5	150.1
540	84.3	53.2	95.8	62.6	57.0	25.5	165.5
294	54.9	52.6	58.6	47.1	30.7	14.5	90.4
216	47.3	44.8	34.2	27.6	15.9	7.3	47.2
120	35.7	36.3	23.5	10.7	7.4	1.1	43.1
56	26.3	29.1	11.5	2.6	1.6	.4	25.1
32	22.8	25.0	8.2	.3	.2	.1	15.7
0	18.1	21.5	4.1	.4	.0	.0	9.5
							7.6
							5.7

Table 20. Ion Density 2×100 (number/cm³)

DAILY AD	LOCAL TIME	7.5	10.5	13.5	16.5	19.5	AVERAGE
1280	1.5	4.5	7.5	10.5	13.5	16.5	22.5
1556	456.8	373.2	521.5	485.1	241.0	121.3	827.1
1656	269.1	225.9	291.7	272.0	148.7	103.3	303.1
1856	196.2	166.3	201.5	188.4	111.7	84.5	216.1
540	147.3	124.0	138.1	123.6	85.0	57.9	155.7
294	115.2	93.2	108.4	93.2	67.7	57.7	119.8
216	95.1	82.3	75.2	68.9	55.6	50.9	94.3
120	84.2	72.4	61.2	54.4	46.3	45.9	74.1
56	76.3	66.2	52.0	45.4	43.2	44.0	80.4
32	74.2	63.7	48.6	41.0	41.3	42.9	71.1
0	70.7	60.5	44.0	37.1	38.6	41.4	67.6
							63.0
							50.5

Table 21. Electron Temperature 2 (eV)

DAILY AP	1.5	4.5	7.5	10.5	13.5	16.5	19.5	AVERAGE
3200	5251.3	13257.6	5473.9	7390.8	9777.3	11237.9	6457.3	22.5
1556	4708.4	9082.5	5536.7	7443.4	9764.6	11265.5	6696.2	3029.6
1056	4397.4	7095.7	5604.7	7506.5	9777.3	11301.7	6973.3	3183.4
640	4159.7	5742.0	5725.8	7622.4	9765.8	11363.2	7492.0	3363.0
384	4081.3	5060.7	5918.4	7827.5	9751.0	11497.1	8438.8	3678.9
216	4127.3	4790.5	6252.5	8261.3	9738.5	11677.7	10582.2	4189.9
120	4271.7	4779.8	6751.3	9197.9	9773.7	12677.3	16121.0	5095.7
56	4494.7	4899.5	7610.8	12990.1	10490.5	19593.3	20000.0	6500.4
32	4631.5	4932.7	8298.1	29003.7	20000.0	20000.0	20000.0	9135.7
								11510.5
								14804.6

Table 22. Ion Temperature 2 (eV)

DAILY AP	1.5	4.5	7.5	10.5	13.5	16.5	19.5	AVERAGE
3200	11458.1	9365.6	7267.2	8589.4	9781.0	5945.1	8486.1	22.5
1656	11145.4	9276.1	7484.5	8657.0	9648.4	6968.0	8634.1	10715.2
1056	10854.3	9210.5	7703.6	8743.8	9586.5	7649.3	8771.5	10548.2
640	10457.3	9136.6	8088.6	8893.6	9577.1	8329.2	8953.7	10398.1
384	10035.1	9065.6	8363.3	9105.0	9642.4	8909.3	9155.9	10169.4
216	9573.4	8937.6	8763.5	9387.1	9780.7	9417.1	9375.4	9920.2
120	9137.3	8945.7	9114.2	9671.4	9839.5	9787.0	9562.9	9545.0
56	8850.1	8903.1	9434.5	9961.8	10106.2	10085.4	9732.2	9408.6
32	8711.3	8884.9	9580.6	10104.3	10187.6	10212.0	9809.0	9196.1
0	8430.1	8952.5	9804.2	10335.4	10317.4	10396.8	9926.7	9170.4
								8955.0
								9573.8
								9635.5

amplitude and local time. The agreement is also quite good for the energy flux and number flux for the electrons, but not as good with the density and pressure (the model predicts two peaks - one near midnight and the other near 0930 in contrast to their single peak near midnight). In consideration of the greater variability of the electrons, this discrepancy is probably a real deviation.

Although skewed somewhat by the problems discussed in earlier sections of the paper (that is, injections and a less than random selection of events), the amplitudes of the four moments predicted by the model for the electrons and ions demonstrate consistent local time variations. For example, all show a sharp minimum between 1630 to 1930 local time for moderate to high levels of geomagnetic activity - the minima being on the order of 50 percent of the maximum values. At low values of geomagnetic activity and for the derived quantities, this trend is lost or greatly reduced. The minimum is obvious in most spectrograms returned by ATS-5 and ATS-6 and probably reflects the sharp edge of the plasma sheet/injection boundary in the evening hours reported by many others^{11, 12, 13} which marks the boundary between eastward drifting low energy ions and westward drifting high energy ions.

In contrast to the minima, the peaks at high geomagnetic activity appear broad in extent and well-defined. At low levels of A_p , all moments peak between 0130 and 0430. The mean energies for the electrons are about one-fourth of expected values and show no strong local time or A_p variation, although there may be a slight tendency for higher energies to occur, on the average near 0430 local time. The mean ion energies, in comparison, peak near midnight moving to earlier hours (~ 2000) as the geomagnetic activity decreases. Again, this would be consistent with the movement of the hot plasma sheet/injection boundary toward the evening hours at geosynchronous orbit during geomagnetic activity.

The derived quantities (mean energy, N_1 , N_2 , T_1 , and T_2), although contaminated by minimum value estimates below $A_p \sim 56$, reveal several features. As just described, the electron mean energy shows no strong variation with local time or A_p . This is consistent with the observations of ATS-5 data reported by

11. Vasyliunas, V. M. (1968) A survey of low energy electrons in the evening sector of the magnetosphere with Ogo 1 and Ogo 3. J. Geophys. Res., 73:2839.
12. McIlwain, C. E. (1971) Plasma convection in the vicinity of the geosynchronous orbit, Earth Magnetospheric Processes, B. M. McCormac, Ed., D. Reidel Publishing Co., Dordrecht, Holland.
13. Mauk, B., and McIlwain, C. E. (1974) Correlation of K_p with the substorm-injected plasma boundary. J. Geophys. Res., 79:3193.

Inouye.¹⁴ The estimates of the standard deviations of these values are on the order of ~ 1500 eV for the electrons and ~ 2000 eV for the ions, quantities of similar magnitude for the electrons as the change in the predicted values. This trend is evident in the 2 Maxwellian fits except, interestingly, the high energy temperature component of the electrons and ions. For them a trend toward higher values for the daily average temperature at lower levels of geomagnetic activity is significant and in contrast to the increase in the daily average of all other parameters. This would lend support to the assumption of Inouye¹⁴ and Stevens et al⁷ that the plasma temperature goes up as the current goes down. The results imply, however, that the effect is dependent on how one defines the energy or temperature. The mean energy as defined in this study is $\sim 1/4$ of its expected value and usually increases. In fact, the temperature as represented by T_2 for the electrons and ions, not the mean energy, better represents the maximum values estimated by other studies.^{7, 4, 15} Also, the maximum temperature and mean energy for the electrons are a factor 2 higher if maximum instead of average values are used in the study.

On the assumption that the 2 Maxwellian fit is a reasonable approximation to the actual plasma distribution, further observations can be made based on the model: First, it is the low temperature component (T_1) of the ions and electrons which shows the largest percentage increase as geomagnetic activity increases. Related to this is the observation that although the densities N_1 and N_2 increase markedly with geomagnetic activity, the ratio, N_2/N_1 of the daily averages of the densities remain roughly equal in spite of large local time variations in the ratios. This may indicate that the percentage of particles, as represented by their ratio N_2/N_1 , in the two populations changes little on a daily basis, whereas their temperatures T_1 and T_2 are varying independent of each other (in fact, the high temperature components may be decreasing with geomagnetic activity). In consideration of the paucity of data in the analysis, however, these conclusions are tentative.

6. MODEL USAGE

In this section, two examples of model usage in estimating the effects of charging will be given. The model will be employed in estimating the environment

14. Inouye, G. T. (1976) Spacecraft potentials in a substorm environment, AIAA Progress in Astronautics and Aeronautics Series, Vol. 42, pp. 103-120.

15. DeForest, S. E. (1977) Final Report for 1 June 1976-30 November 1976, AFGL-TR-77-0031.

conducive to charging at geosynchronous orbit. * This environment can, in turn, be joined with a spacecraft charging model to give satellite potentials.

Of general interest is the prediction of the charging environment a satellite is likely to encounter during a typical mission. The basic idea is to predict the expected occurrence frequency of A_p during the mission. This has been done for a "typical" time period in Figure 3 where a histogram of over 30 years of A_p values has been plotted. The results of this figure can be utilized in two ways. First, the probability of observing a given interval of A_p or, equivalently, a given level of geomagnetic activity can be found; for example, the probability of observing the A_p interval 56-120 is 33 percent in a given time period. Similarly, the probability that a value of A_p of 120 will be exceeded during a mission is given by:

$$P = 100\% - 14\%(A_p \leq 32) - 23\%(32 < A_p \leq 56) \\ - 33\%(56 < A_p \leq 120) = 30\%$$

The value of A_p (120 in this example) can then be substituted into the model (see Appendices for a FORTRAN listing of the model) along with a local time between 0000 and 2400 to give the ambient environment expected 33 percent of the time, or not to be "exceeded" more than 30 percent of the time.

Substituting the A_p value of 120 and a LT of 0130, the FORTRAN subroutine returns, * one notes:

	<u>Electron Population</u>	<u>Ion Population</u>
Number density (no#/cm ³)	1.49	1.38
Pressure (dynes/cm ²)	3.31×10^{-9}	1.24×10^{-8}
Energy flux (erg/cm ² sec-sr)	1.89	0.30
Number flux (no#/cm ² sec-sr)	2.57×10^8	10^7
Mean energy 3/2 kT (eV)	2100	8400
Current (amps/cm ²)	0.13	0.005

* The model is not intended to be used to give total average plasma "dosages" since plasma injections occurring when the satellite was near local midnight were preferentially selected. Rather, it is intended to give the environment most conducive to charging - that is, following injections when the satellite is near local midnight.

* Note: These values are in very good agreement with DeForest and McIlwain⁵ and Garrett et al⁴ for "typical" values if 3/2 (T_2) is the "mean energy."

	<u>Electron Population</u>	<u>Ion Population</u>
2 Maxwellian:		
N1 (no#/cm ³)	1.13	0.54
T1 (eV)	496	21
N2 (no#/cm ³)	0.35	0.84
T2 (eV)	4270	9200

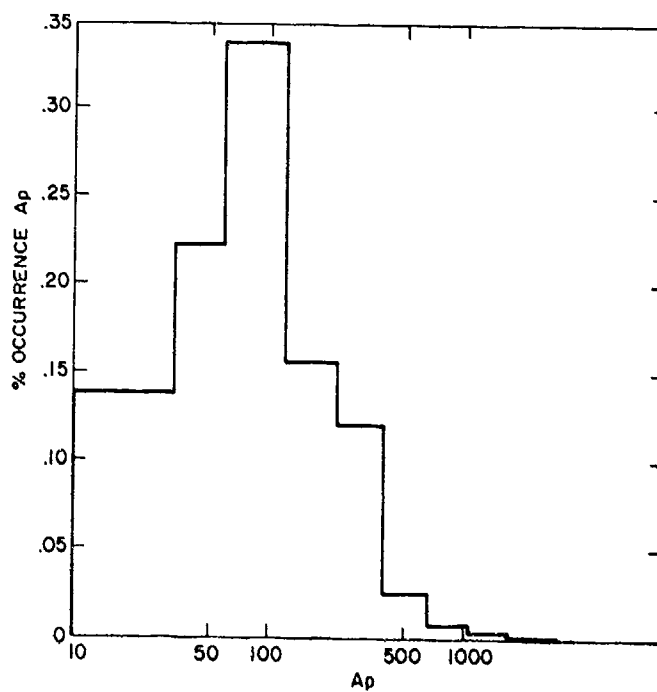


Figure 3. Histogram of the Occurrence Frequency of A_p , the Daily Sum of a_p , for the Years 1932 through 1975

The approximate distribution function (or particle spectrum) can then be derived by either of the following:

Electrons

$$f_e(E) = 27.2 N_e \left(\frac{T_e}{1000} \right)^{-3/2} e^{-E/T_e} \quad (12a)$$

Ions

$$f_I(E) = 2.14 \times 10^6 N_I \left(\frac{T_I}{1000} \right)^{-3/2} e^{-E/T_I} \quad (12b)$$

where

f_e, f_I = distribution functions ($\text{sec}^3 \text{ km}^{-6}$)

$$N_e = 1.49 \text{ cm}^{-3}$$

$$N_I = 1.38 \text{ cm}^{-3}$$

$$T_e = 2/3 (2100 \text{ eV}) = 1400 \text{ eV}$$

$$T_I = 2/3 (8400 \text{ eV}) = 5600 \text{ eV}$$

E = particle energy (eV)

or:

$$f'_e(E) = 27.2 \left(N1_e \left(\frac{T1_e}{1000} \right)^{-3/2} e^{-E/T1_e} + N2_e \left(\frac{T2_e}{1000} \right)^{-3/2} e^{-E/T2_e} \right) \quad (13a)$$

$$f'_I(E) = 2.14 \times 10^6 \left(N1_I \left(\frac{T1_I}{1000} \right)^{-3/2} e^{-E/T1_I} + N2_I \left(\frac{T2_I}{1000} \right)^{-3/2} e^{-E/T2_I} \right) \quad (13b)$$

where

f'_e, f'_I = distribution functions ($\text{sec}^3 \text{ km}^{-6}$)

$$N1_e = 1.13 \text{ cm}^{-3} \quad N1_I = 0.54 \text{ cm}^{-3}$$

$$T1_e = 496 \text{ eV} \quad T1_I = 21 \text{ eV}$$

$$N2_e = 0.35 \text{ cm}^{-3} \quad N2_I = 0.84 \text{ cm}^{-3}$$

$$T2_e = 4270 \text{ eV} \quad T2_I = 9200 \text{ eV}$$

The resulting distribution functions are plotted in Figures 4 and 5. It is recommended that Eq. (13) be used for A_p greater than 50, and Eq. (12) for lower values.

A second use of the model is in making real time estimates of the plasma conditions. A provisional a_p value and a predicted a_p value for the next 3-hour period are currently available from Air Force sources. If a running sum of a_p 's is maintained, the model can be used to predict the ambient conditions (that is, if

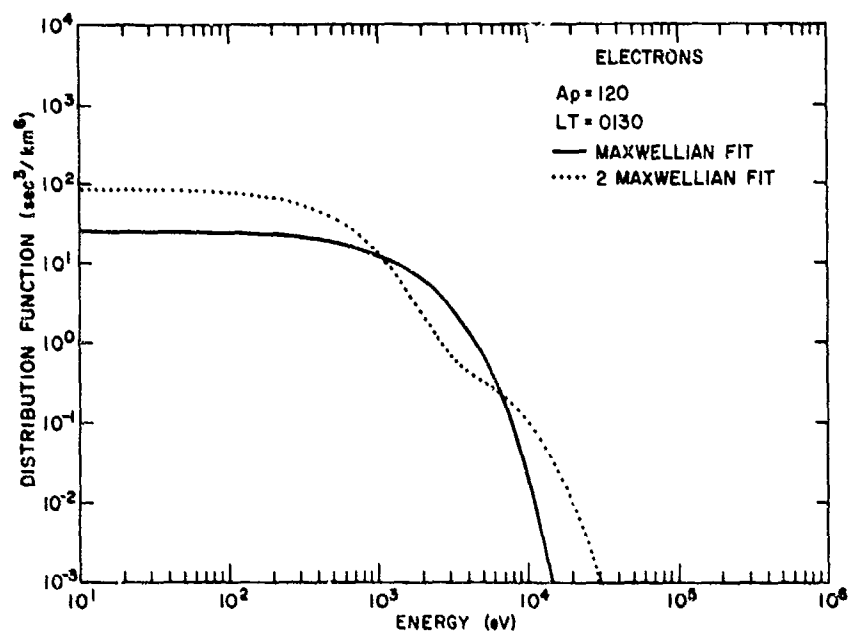


Figure 4. Maxwellian and 2 Maxwellian Electron Distribution Functions Predicted by the Model for A_p of 120 and a Local Time of 0130

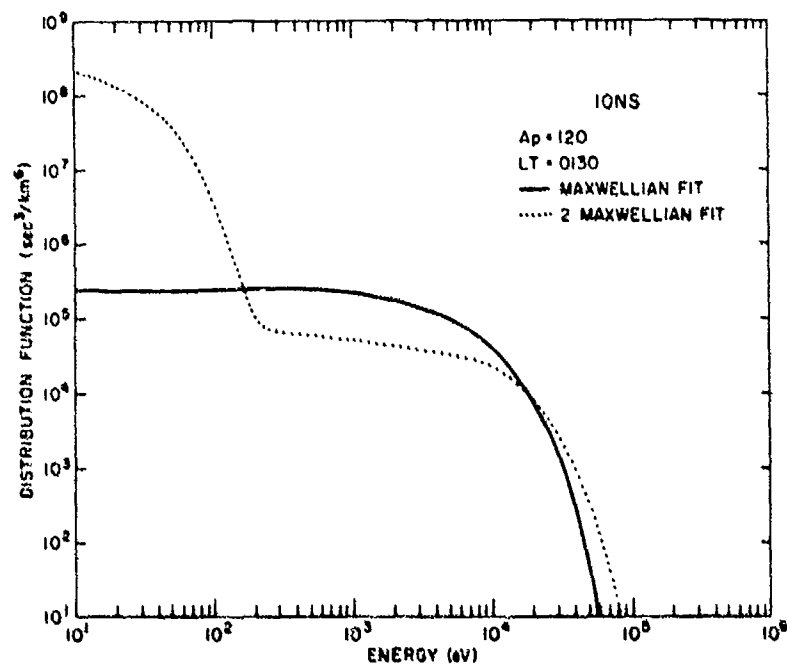


Figure 5. Maxwellian and 2 Maxwellian Ion Distribution Functions Predicted by the Model for A_p of 120 and a Local Time of 0130

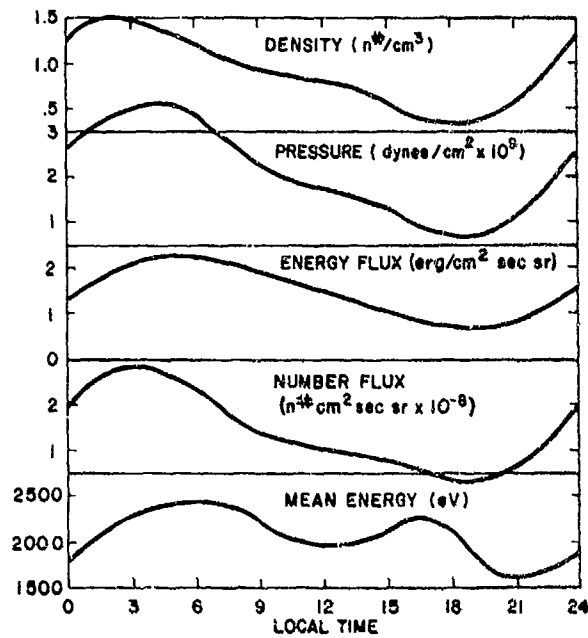


Figure 6. Local Time Plot of the Values of the Four Electron Moments Predicted by the Model for A_p of 120

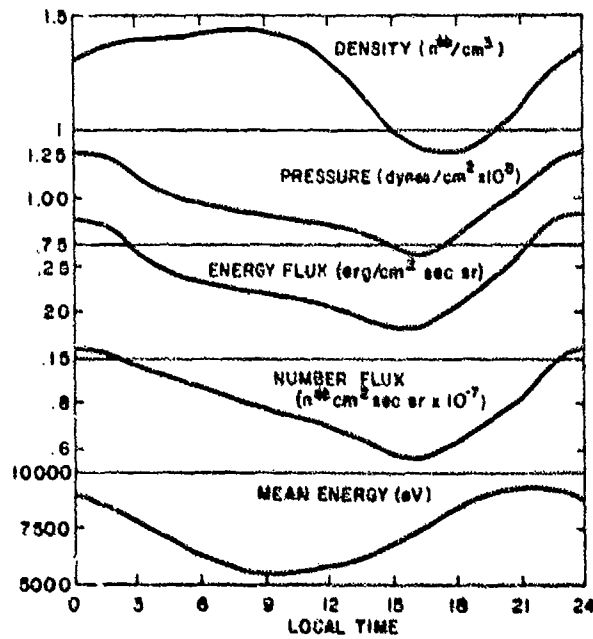


Figure 7. Local Time Plot of the Values of the Four Ion Moments Predicted by the Model for A_p of 120

the preceding 7 a_p values totaled 105 and the predicted a_p was 15, then A_p predicted would be 120 and the environment versus local time for the next three hours would be as shown in Figures 6 and 7). Likewise, if the current A_p value is 120, Figures 6 and 7 illustrate the average conditions following an injection near the local midnight portion of a satellite's orbit, the condition most likely to foster charging. Extreme conditions, suitable for providing a spacecraft charging alert, are estimated by taking the largest observed or predicted a_p value in the desired interval and multiplying by 8 (if the highest a_p was 15, then A_p predicted would be 120). The values so derived can then be inserted in a program that computes spacecraft potential to give an "alert" bulletin versus local time.

7. CONCLUSION

In review, we have outlined a procedure for generating an analytic formulation of the various parameters needed by researchers seeking to model the geosynchronous environment and the interaction of that environment with a spacecraft. An environmental model based on a limited data set (10 days) was analyzed under this procedure. The results were compared with other observations of the geosynchronous plasma. Although the model was designed to analyze plasma variations following a plasma injection near the midnight portion of the satellite orbit, excluding anisotropic fluxes and orbital effects, it included geomagnetic and local time variations. Key features of the magnetosphere such as the plasma decrease near evening were reproduced, and various trends in the data which may be significant noted. In view of the assumptions and size of the data base, this model is considered to be a preliminary rather than a definitive description of the ambient geosynchronous environment. As the power of the technique has been demonstrated, it is planned to extend it in the near future to a much more comprehensive data base and, in turn, generate a more complete model.

References

1. DeForest, S.E. (1972) Spacecraft charging at synchronous orbit, J. Geophys. Res. 77(No. 4):651.
2. McPherson, D.A., Cauffman, D.P., and Schober, W. (1975) Spacecraft Charging at High Altitudes - The SCATHA Program, AIAA paper, pp. 75-92.
3. Pike, C., and Bunn, M.H. (1976) A correlation study relating spacecraft anomalies to environmental data, Spacecraft Charging by Magnetospheric Plasma, AIAA Progress in Astronautics and Aeronautics Series, Vol 42.
4. Garrett, H.B., Pavel, A.L., and Hardy, D.A. (1977) Rapid Variations in Spacecraft Potential, AFGL-TR-77-0132.
5. DeForest, S.E., and McIlwain, C.E. (1971) Plasma clouds in the magnetosphere, J. Geophys. Res. 76(No. 16):3587-3611.
6. Reasoner, D.L., Lennartsson, W., and Chappell, C.R. (1976) Relationship between ATS-6 spacecraft-charging occurrences and warm plasma encounters, Spacecraft Charging by Magnetospheric Plasmas, AIAA Progress in Astronautics and Aeronautics Series, Vol. 42.
7. Stevens, N.J., Lovell, R.R., and Purvis, C.K. (1977) Provisional specification for satellite time in a geomagnetic substorm environment, Proc. of the Spacecraft Charging Conference, AFGL-TR-77-0051/NASA-TMX-73537.
8. Su, S.-Y., and Konradi, A. (1977) Description of the Plasma Environment at Geosynchronous Altitudes, to be published as NASA-Johnson Note P-10.
9. Rostoker, G. (1972) Geomagnetic indices, Rev. Geophys. 10(No. 4):935.
10. Bevington, P.R. (1969) Data Reduction and Error Analysis for the Physical Sciences, McGraw-Hill, New York.
11. Vasyliunas, V.M. (1968) A survey of low energy electrons in the evening sector of the magnetosphere with Ogo 1 and Ogo 3, J. Geophys. Res., 73:2839.

12. McIlwain, C.E. (1971) Plasma convection in the vicinity of the geosynchronous orbit, Earth Magnetospheric Processes, B.M. McCormac, Ed., D. Reidel Publishing Co., Dordrecht, Holland.
13. Mauk, B., and McIlwain, C.E. (1974) Correlation of K_p with the substorm-injected plasma boundary, J. Geophys. Res. 79:3193.
14. Inouye, G.T. (1976) Spacecraft potentials in a substorm environment, AIAA Progress in Astronautics and Aeronautics Series, Vol. 42, pp. 103-120.
15. DeForest, S.E. (1977) Final Report for 1 June 1976-30 November 1976, AFGL-TR-77-0031.
16. Akasofu, S.-I., and Chapman, S. (1972) Solar-Terrestrial Physics, Clarendon Press, Oxford.

Appendix A

Calculation of Moments

The ATS-5 UCSD instrument makes measurements only between 51.6 eV and 51.6 keV. Further, all positive ions are assumed to be ionized hydrogen as it is not possible to calculate accurately the composition of the ion population. Thus, the four moments calculated from the ATS-5 data are in actuality valid only for the range 51.6 eV to 51.6 keV for electrons and protons. DeForest¹ notes that the main error introduced by these effects is an underestimation of the particle density and a lack of equality between the proton and electron densities as a large part of the particle population is below 50 eV. With this in mind, the formulas for the moments in Eqs. (5), (6), (7), and (8) are approximated for the electrons by:

$$\langle N_e \rangle = 4\pi \sum_{E_i} \left. \frac{d(EF)}{dE} \right|_i \left(\frac{2E_i}{M_e} \right)^{-1/2} \frac{\Delta E_i}{E_i} \quad (1A)$$

$$\langle NF_e \rangle = \sum_{E_i} \left. \frac{d(EF)}{dE} \right|_i \frac{\Delta E_i}{E_i} \quad (2A)$$

$$\langle P_e \rangle = 4\pi \sum_{E_i} \left(\frac{m_e}{2} \right) \frac{d(EF)}{dE} \bigg|_i \left(\frac{2E_i}{m_e} \right)^{1/2} \frac{\Delta E_i}{E_i} \quad (3A)$$

$$\langle EF_e \rangle = \sum_{E_i} \left(\frac{m_e}{2} \right) \frac{d(EF)}{dE} \bigg|_i \left(\frac{2E_i}{m_e} \right) \frac{\Delta E_i}{E_i} \quad (4A)$$

where

\sum_{E_i} = summation over the energies E_i from 51.6 eV to 51.6 keV

m_e = mass of electron

$\frac{d(EF)}{dE} \bigg|_i$ = differential energy flux (count rate divided by $4.3 \times 10^{-5} \text{ cm}^2 \text{ sr}$ for ATS-5)

$\frac{\Delta E_i}{E_i}$ = 0.12 for ATS-5

The ion moments are similarly derived by replacing m_e by m_i , the mass of a proton.

Appendix B

Calculation of the 2 Maxwellian Distribution

The distribution function f is of central importance in various schemes for the calculation of spacecraft potential. As Figure 1 clearly demonstrates, a single Maxwellian distribution is often inadequate in describing the actual data. Although a 2 Maxwell fit is also only an approximation, it does double the knowledge of the actual distributions. Further, it tends to divide the particle distribution into two components: a high temperature, relatively low density component and a low temperature, high density component which is consistent with various observations of the actual state of the magnetospheric plasma. For these reasons, to include the calculation of the two densities (N_1 and N_2) and temperatures (T_1 and T_2) in the model was warranted.

Assuming a 2 Maxwellian distribution to be given by Eq. (9) and making the additional assumption that the four moments given in Appendix A represent adequate approximation to the actual distribution function, we obtain:

$$N_1 + N_2 = C_1 \quad (5A)$$

$$N_1 X_1 + N_2 X_2 = C_2 \quad (6A)$$

$$N_1 X_1^2 + N_2 X_2^2 = C_3 \quad (7A)$$

$$N_1 X_1^3 + N_2 X_2^3 = C_4 \quad (8A)$$

where

$$\begin{aligned}
 N_1, N_2 &= \text{number densities for species } i \\
 X_1 &= T_{1i}^{1/2}, \text{ temperature 1 for species } i \\
 X_2 &= T_{2i}^{1/2}, \text{ temperature 2 for species } i \\
 C_1 &= \langle n_i \rangle \\
 C_2 &= \langle NF_i \rangle \\
 C_3 &= \langle P_i \rangle / K \\
 C_4 &= \langle EF_i \rangle
 \end{aligned}$$

Solving:

$$N_1 = C_1 - N_2 \quad (9A)$$

$$N_2 = \frac{C_2 - X_1}{X_2 - X_1} \quad (10A)$$

$$X_2 = \frac{C_3 - C_2 X_1}{C_2 - C_1 X_1} \quad (11A)$$

$$(C_2^2 - C_1 C_3) X_1^2 + (C_1 C_4 - C_2 C_3) X_1 + (C_3^2 - C_2 C_4) = 0 \quad (12A)$$

Equation (12A) is a quadratic equation and has two roots of the form:

$$X_1 = \frac{-B + \sqrt{B^2 - 4AC}}{2A} \quad (13A)$$

$$X_1 = \frac{-B - \sqrt{B^2 - 4AC}}{2A} \quad (14A)$$

where

$$\begin{aligned}
 A &= C_2^2 - C_1 C_3 \\
 B &= C_1 C_4 - C_2 C_3 \\
 C &= C_3^2 - C_2 C_4
 \end{aligned}$$

This situation may appear ambiguous, but it is obvious by the symmetry of Eqs. (5A), (6A), (7A), and (8A) that if we choose the positive sign for X_1 , then X_2 must correspond to the negative sign. The actual problem is that it is possible that the distribution function is a single Maxwellian in which case X_2 (or by symmetry, X_1) will approach infinity and the number density, N_0 , zero. Some care must be exercised in studying trends as a result of this effect.

For actual data, it is not likely that imaginary or negative values will be encountered. For values derived from our simple model, this is not true: The fitted moments may be negative (in which case imaginary values are obtained), or the minimum correction values may result in negative densities. Fortunately, this happened for only 7 of the 80 values calculated for the electrons; it did not occur for the ions. Default values representative of the expected minimum values are returned by the program in these cases (see Appendix C). Finally, $T_{1i}^{1/2}$ or $T_{2i}^{1/2}$ may be negative and should be checked in any general application.

Appendix C

FORTTRAN Listing of Environmental Model

The model outlined in this study consists of two subroutines: MODEL and MAXW. These two programs have separate purposes and can, with minor changes, be used independently.

Subroutine MODEL requires as input the daily A_p index and the local time LT (a real number). It returns a vector XX which has the 20 components:

- XX(1) = Electron density $\times 100$ (number/cm³)
- XX(2) = Ion density $\times 100$ (number/cm³)
- XX(3) = Electron pressure $\times 10^{10}$ (dynes/cm²)
- XX(4) = Ion pressure $\times 10^{10}$ (dynes/cm²)
- XX(5) = Electron energy flux $\times 100$ (erg/cm² sec-sr)
- XX(6) = Ion energy flux $\times 100$ (erg/cm² sec-sr)
- XX(7) = Electron number flux $\times 10^{-6}$ (number/cm² sec-sr)
- XX(8) = Ion number flux $\times 10^{-6}$ (number/cm² sec-sr)
- XX(9) = Electron mean energy (eV)*
- XX(10) = Ion mean energy (eV)*

* Mean energy, which is $3/2 KT$ for a Maxwellian, should not be confused with the temperature, KT , used in generating the Maxwellian or 2 Maxwellian distribution.

XX(11) = Electron current $\times 10^4$ (n amps/cm²)
 XX(12) = Ion current $\times 10^4$ (n amps/cm²)
 XX(13) = Electron density 1×100 (number/cm³)
 XX(14) = Ion density 1×100 (number/cm³)
 XX(15) = Electron temperature 1 (eV)
 XX(16) = Ion temperature 1 (eV)
 XX(17) = Electron density 2×100 (number/cm³)
 XX(18) = Ion density 2×100 (number/cm³)
 XX(19) = Electron temperature 2 (eV)
 XX(20) = Ion temperature 2 (eV)

Subroutine MODEL requires MAXW but it can easily be deleted if the 2 Maxwellian distribution is not required. Subroutine MAXW requires a set of four moments:

RHO = density (number/cm³)
 FNO = number flux (number/cm²-sec-sr)
 PR = pressure (dynes/cm²)
 FEN = energy flux (erg/cm²-sec-sr)

A value of 1 is used for electrons, 2 for ions. It returns:

R1 = density 1 (number/cm³)
 Y = temperature 1 (eV)
 R2 = density 2 (number/cm³)
 T = temperature 2 (eV)

These values can be used in Eq. (9) to give an approximation to the distribution function.

Table 2 of the main report gives default values returned by the program. These are the most reasonable estimates of these values that could be determined.

```

SUBROUTINE MODEL (AP,LT,XX)
DIMENSION XX(10),X(10),XX(20)
REAL LT
DATA ((X(I,J),I=1,10),J=1,8)/
1 .3835E+02,-.4166E+02, .2184E+02,-.2101E+01,-.7312E+02,
1 .4255E+00,-.7337E-01,-.5953E-01,-.8828E-01,-.4436E-01,
1 .9853E+02,-.2720E+02, .2276E+01,-.2758E+01,-.3287E+01,
1 .2980E+00,-.9757E-02,-.3543E-01,-.4836E-01,-.3773E-01,
1 .5195E+01,-.1036E+02, .6420E+01, .2609E+01,-.4776E+01,
1 .1253E+00,-.2784E-01,-.3329E-01,-.2831E-01,-.2257E-02,
1 .7684E+02,-.4464E+01, .1610E+02,-.8089E+00,-.3110E+01,
1 .1628E+01,-.4942E-01,-.4189E-01,-.6374E-01,-.2369E-01,
1 .3579E+02,-.7375E+02, .5046E+02, .2135E+02,-.1075E+02,
1 .9136E+00,-.3251E-01,-.5064E+00,-.1706E+00,-.4715E-01,
1 .1858E+02,-.5158E+00, .3109E+01,-.6267E-01,-.5042E+00,
1 .3776E-01,-.1237E-01, .1490E-01,-.1782E-01,-.7398E-02,
1 .4719E+02,-.6769E+02, .3818E+02, .7563E+01,-.4420E+02,
1 .8101E+00,-.2435E+00,-.4471E-01,-.1109E+00,-.5880E-01,
1 .6232E+01,-.9452E+00, .1427E+01,-.1282E+00,-.3729E+00,
1 .1479E-01,-.3372E-02, .7584E-03,-.4736E-02,-.2516E-02/
DATA (X(1,I),I=1,8)/2.0,33.,.4,40.,8.,9.,4.,3./
FLAG=0
DO 2 I=1,8
XX(I)=0
DO 1 J=1,8
IPA=J/5
IPT=J-5*I*4
Y=1
X1=(LT+6.5)/3.
TPI=6.28318
IF (IPT.EQ.1) Y=COS(X1*TPI/8.)
IF (IPT.EQ.2) Y=SIN(X1*TPI/8.)
IF (IPT.EQ.3) Y=COS(X1*TPI/4.)
IF (IPT.EQ.4) Y=SIN(X1*TPI/4.)
J1=J+1
1 XX(I)=(AP+Y*IPA)*XX(J1,I)+XX(I)
XX(I)=XX(I)+X(1,I)
IF (XX(I).LT.XMIN(I)) FLAG=1
2 IF (XX(I).LT.XMIN(I)) XX(I)=XMIN(I)
XX(9)=XX(3)*9360./XX(1)
XX(10)=XX(4)*9360./XX(2)
XX(11)=XX(7)*1.6*3.14159
XX(12)=XX(9)*1.6*3.14159
DO 3 I=1,2
K=I-1
RHO=XX(K+1)/100.
FNO=XX(K+7)*1.E+06
PR=XX(K+3)/1.E+10
FEN=XX(K+5)/100.
CALL VAXH(RHO,FNO,PR,FEN,A,B,C,D,I)
XX(K+13)=A*100.
XX(K+15)=B
XX(K+17)=C*100.
3 XX(K+19)=D
IF (XX(15).LT.200.) GO TO 5
IF (FLAG.EQ.1) GO TO 4

```

```

5 XX(9)=1000
  XX(13)=XX(1)
  XX(15)=25.
  XX(17)=XX(1)/50.
  XX(19)=2*000
4 CONTINUE
  RETURN
  END

```

```

SUBROUTINE MAXW(RHO,FNO,PR,FEN,R1,Y,R2,T,I)
0 Y=1 IS FOR ELECTRONS. I=2 IS FOR IONS
  DIMENSION X(2),Z(2)
  X(1)=2.022E-05
  X(2)=8.05E-04
  Z(1)=7.32E+10
  Z(2)=3.14E+12
100 FORMAT(4(1X,E17.6))
101 FORMAT(1X,*IMAGINARY*)
  C1=RHO
  C2=FNO*Y(I)
  C3=PR/1.38E-16
  C4=FEN*Z(I)
  A=C2*C2-C1*C3
  B=C1*C4-C2*C3
  D=C3*C3-C2*C4
  D=B*B-4.*A*C
0 CHECKS FOR IMAGINARY ROOT
  IF (D.LT.0.0) GO TO 99
  Y=((-B+SQRT(D))/(2.*A))
C CHECKS FOR PROPER ROOTS
  G=((-D+SQRT(D))/(2.*A))
  T=(C3-C2*Y)/(C2-C1*Y)
  IF (ABS(T)-1.LT..01) GO TO 98
  PRINT 101,Y,T,G
98 CONTINUE
  R2=(C2-Y*C1)/(T-Y)
  R1=C1-R2
  Y=Y*Y/1.15E+04
  T=T*T/1.16E+04
  G=G*G/1.16E+04
  RETURN
99 PRINT 101
  PRINT 100,A,B,C,G,C1,C2,C3,C4
  A=R1,R2
  END

```